Recent Advances in Strong Ground Motion Prediction

Paul Somerville [1]

ABSTRACT

Current ground motion attenuation relations predict ground motion parameters using a simplified model in which the effects of the earthquake source are represented by earthquake magnitude; the effects of wave propagation from the earthquake source to the site region are specified by a distance; and the effects of the site are specified by a site category. These ground motion models have a large degree of uncertainty because other conditions that are known to have an important influence on strong ground motions, such as near-fault rupture directivity effects, crustal waveguide effects and basin response effects, are not treated as parameters of these simple models. In order to reduce the uncertainty in ground motion prediction at a given site, we need to augment this parameterization of ground motion models to include more realistic representations of source, path and site effects. This paper describes the application of seismological methods to the development of more realistic and more accurate ground motion prediction models.

EMPIRICAL GROUND MOTION ATTENUATION RELATIONS

During the past decade, large sets of strong motion recordings were obtained from numerous earthquakes, significantly expanding the data base of strong motion recordings available for the derivation of empirical ground motion models. A collection of recent models based on recorded data and in some cases on seismological models, accompanied by an overview (Abrahamson and Shedlock, 1997), was published in Seismological Research Letters. These ground motion models are for distinct tectonic categories of earthquakes: shallow crustal earthquakes in tectonically active regions; shallow crustal earthquakes in tectonically stable regions; and subduction zone earthquakes. Subduction zone earthquakes are further subdivided into those that occur on the shallow plate interface, and those that occur at greater depths within the subducting plate. Strong ground motions from subduction earthquakes generally attenuate more gradually with distance than crustal earthquakes, and earthquakes occurring with the subducting slab produce stronger ground motions than those occurring on the subduction interface. Mixing these data sets gives rise to attenuation relations that overpredict the ground motions from crustal and shallow subduction earthquakes and underpredict those from deep slab earthquakes.

Some features of recent peak acceleration attenuation relations are summarized as follows. There is a "distance saturation" in which the slope of the attenuation decreases at close distances, reflecting the fact that the earthquake is a distributed source, not a point source. For related reasons, there is a "magnitude saturation" in which the ground motions increase more gradually with magnitude for large magnitudes. At large distances, the ground motions are typically larger on soil sites than on rock sites, reflecting the effect of amplification due to impedance contrast. However, at close distances where ground motion levels are high, the non-linear behavior of soils tends to offset the impedance contrast effects, to the extent that high frequency ground motions on rock may exceed those on some soils at very close distances to large earthquakes.

Parameters of Simple Empirical Ground Motion Models

The simplest ground motion attenuation relations predict ground motion parameters using a simplified model in which the effects of the earthquake source are represented by earthquake magnitude; the effects of wave propagation from the earthquake source to the site region are specified by a distance; and the effects of the site are specified by a site category (Table 1). Other conditions that are known to have an important influence on strong ground motions, such as near-fault rupture directivity effects and basin response effects, are generally not specifically included in such ground motion prediction models. Consequently, existing methods tend to underestimate the ground motions where these conditions are present, and overestimate them where these conditions are absent.

[1] URS Greiner Woodward Clyde, Pasadena, CA, USA.

Moment magnitude is the most appropriate measure of earthquake size, because it is directly related to the seismic moment of the earthquake, and thus to the fault area and the average displacement on the fault. Moment magnitude can thus be directly related to measures of strain rate, such as the slip rate of a specific fault. When earthquake occurrence rates are instead based on historical seismicity in seismic hazard analyses, other magnitude measures are sometimes used because the seismic moments of the historical earthquakes may be poorly known.

There is a well established difference in ground motion amplitudes between reverse and strike-slip faulting mechanisms for crustal earthquakes in empirical ground motion attenuation relations. In these models, ground motions for reverse earthquakes typically exceed those for strike-slip earthquakes by a factor ranging from about 1.3 to 1.4. In some models, these differences are magnitude dependent. Although no definitive explanation of this difference has been identified, there is a preliminary indication that it may be attributable to differences in dynamic parameters, specifically the rise time (duration of slip) at a point on the fault (Somerville and Sato, 1998). For a given seismic moment, the rise times for reverse earthquakes are on average about half as long as those for strike-slip earthquakes. Strong motion simulations show that halving the rise time causes an increase of about a factor of 1.4 in ground motion amplitudes. This increase is consistent with the style of faulting factor in empirical strong motion attenuation relations. Available data indicate that strong motion data from normal faulting earthquakes are several tens of percent lower than those for strike-slip earthquakes.

The distance between the source to the site is measured in a variety of different ways, including closest distance to the rupture surface, closest distance to the seismogenic rupture surface, closest distance to the vertical projection of the rupture to the surface, and hypocentral distance, as summarized by Abrahamson and Shedlock (1997). The lack of a standard definition of distance hinders the comparison and use of multiple ground motion attenuation relations, which is necessary to fully account for uncertainty in estimated ground motions.

Site categories are usually based either on geological criteria or on shear wave velocity of the surficial materials. The use of shear wave velocity has the advantage of being based on an objective measure which affects ground motions in a way that can be modeled. However, it cannot be directly applied to sites that lack shear wave velocity measurements. Also, deeper geological structure such as sedimentary basins and laterally varying structure may have an equally strong or even stronger effect on site response.

A major shortcoming of existing attenuation relations is the lack of a standard definition of site categories. Consequently, a large source of difference in the ground motion models of different investigators lies in the different criteria that are used for site conditions, and in the assignment of site categories to individual recording sites. The use of a standard site classification system, such as that used in the current NEHRP provisions in the United States, and the assignment of these categories to individual recording stations, has the potential to reduce these unnecessary discrepancies between different model predictions. Also, the important effect of nonlinear soil behavior on site response is recognized in the site response factors that are embodied in current building codes and provisions in the United States (1997 UBC; 1997 NEHRP).

Variability in Ground Motions

The variability in earthquake ground motions has long been recognized and taken into account in engineering applications. There is a large amount of variability in ground motions due to effects that are more complex than the simple parameterization described above based on magnitude, distance and site category. New methods for analyzing the origins of this variability have provided important insight into the nature of strong ground motions, and indicate the directions in which further research may be able to reduce the uncertainty in the estimation of ground motions for engineering application. Specifically, the random effects approach (Abrahamson and Youngs, 1992) has been applied to the strong motion data base to separately quantify two sources of variability: the variability in the average ground motions from one earthquake to the next, and the variability in ground motions from one site to another at the same closest distance from a given earthquake. For earthquakes of a given tectonic category larger than about magnitude 6, the event-to-event variability is found to be insignificant compared with the intra-event variability (Youngs et al., 1995). The overall variability thus decreases significantly for the larger magnitudes. The decrease in the variability of ground motion amplitudes with increasing magnitude can have a significant effect on the probabilistic estimation of ground motions.

This finding indicates that while the average ground motions from one large earthquake are very similar to those of another, there are conditions that cause the ground motions to vary significantly from one location to another at the same distance from a given event. The factors that cause this variability are related to aspects of the earthquake source process, the propagation of seismic waves from the source region to the site region, and the site response that are not contained in the simple magnitude-distance-site category parameterization of standard attenuation relations. In these simple models, these other sources of variability are treated as randomness, whereas they potentially could be treated as resulting from specific effects which may be predictable. While those predictable effects may have uncertainties of their own, in some cases it should be possible to reduce these uncertainties.

For example, current empirical ground motion models are derived from recordings at many sites that fall within a given site category. For a given site category, these models treat site-to-site variability as random. For a given site, strong motion recordings may exist which describe the site response, or a geotechnical boring could potentially be used to characterize the response of the site. Although the site response would still have some uncertainty in these cases, that uncertainty would be less than the standard error of empirical attenuation relations, which represents large site-to-site variations in site response. In this situation, the variability among different sites in the strong motion data set is irrelevant to (and overestimates) the uncertainty in ground motion at the specific site. This is especially important for ground motions having low annual probabilities of exceedance, for which the variability in ground motion is the principal cause of the increase in calculated ground motion level as the annual probability of occurrence decreases. These large calculated ground motion levels in many cases are a reflection of our ignorance of the objective ground motion conditions that exist at a given site rather than an accurate estimate of the potential for large ground motions at the site.

Enhanced Ground Motion Attenuation Models

In order to reduce the uncertainty in predicting the ground motions at a given site, we need to augment our ground motion prediction models to include more realistic representations of source, path and site effects. The focus of this paper is on ways in which the parameterization of conventional ground motions models can be augmented to include important additional factors that strongly influence ground motions. We expect that this augmented parameterization will reduce the uncertainty in predicted ground motions.

During the past decade, the number of parameters used in the estimation of strong ground motion has grown beyond the simple set of magnitude, distance and site category. In addition to magnitude, the additional parameters used to describe the source include faulting style, and parameters that cause spatial variations in the ground motions around a fault due to its geometry and to rupture directivity effects. In place of using simple monotonic models for the attenuation of ground motion with distance, more complex models that take account of seismic wave propagation in a layered crust have been developed. In place of simple geological descriptors of site conditions or ranges of seismic velocity, the complexity of the interaction of waves arriving at the site with the strongly heterogeneous conditions that characterize the shallow geology of most sites has been recognized and analyzed.

One approach to accounting for these effects in ground motion models is to include them in empirical models by using a larger number of predictive parameters related to source, path and site conditions. Examples of this approach are the empirical models of hanging wall effects (Abrahamson and Somerville, 1996) and near-fault rupture directivity effects (Somerville et al., 1997). The former uses a simple geometrical model to distinguish hanging wall sites from other sites, and the latter uses parameters such as the angle between the fault rupture direction and the direction from the earthquake to the site.

Another approach is to use seismologically-based ground motion models that take account of the specific source, path and site conditions. These methods can be used to augment the recorded data used to generate empirical models, or to generate suites of ground motion estimates that can be used to develop independent ground motion models. Ground motion models based on synthetic seismograms can then be used to complement available empirical models. In some regions, such as eastern Canada, the data base of strong motion recordings is too sparse to allow the development of empirical ground motion models. In this case, ground motion attenuation relations are based primarily on seismological models which are described next. Also, considerable progress has been made in understanding and predicting ground motion variability, especially at periods longer than about 1 second, through the modeling of specific effects such as rupture directivity and basin response. In later sections, we describe the use of seismological models to predict ground

motions that include these conditions. If we can incorporate these effects into ground motion models, in addition to the standard parameters of magnitude, distance and site category, we will be able to reduce the uncertainty in the ground motion estimates for a specified site.

GROUND MOTION SIMULATION PROCEDURES

Three alternative procedures for estimating strong ground motion are summarized in Table 1. Empirical ground motion attenuation relations of the kind described above are available for predicting the strong motions from earthquakes in tectonically active regions. However, the data base of strong motion recordings in tectonically stable regions is too sparse to permit the development of empirical attenuation relations based purely on recorded data. This necessitates the use of seismologically based methods to generate ground motion attenuation relations in eastern Canada. The simplest seismologically based method is the Band-Limited White Noise-Random Vibration Theory method (Boore, 1983), often referred to as the stochastic method. This method models ground motion as a time sequence of band limited white noise. A Fourier spectral model of the ground motion is constructed, starting with a model of the source spectrum and modifying its shape by factors to represent wave propagation effects. Current models based on the stochastic method include EPRI (1993); Atkinson and Boore (1995; 1997), and Toro et al. (1997). There is currently debate among proponents of the stochastic method as to whether the source spectrum is best represented by a Brune spectrum with a single corner frequency, or by a model having two corner frequencies (Atkinson, 1993; Boatwright and Choy; 1992).

The broadband Green's function procedure is a more rigorous procedure that contains fewer simplifications than the stochastic model. By using scaling relations for earth quake source parameters in conjunction with the elastodynamic representation theorem, we are able to construct ground motion time histories without resorting to a priori assumptions about the shape of the source spectrum. The Green's functions that are used in this procedure can be calculated from known crustal structure models, facilitating the use of the procedure in regions where recorded data are sparse or absent.

Table 1. Ground Motion Prediction Methods

METHOD	SOURCE	PATH	SITE
EMPIRICAL	Seismic Moment	Distance	Geological category
STOCHASTIC	Source spectrum, e.g. 1 corner (Brune) or 2 corners (Atkinson)	Attenuation function e.g. $1/R$ - $1/R^{1/2}$, or empirical. Duration varies with R. Q.	Kappa or fmax
BROADBAND GREEN'S FUNCTION	Shear dislocation, slip time function specified on fault	Green's functions including body waves, surface waves, Q.	Kappa; empirical or theoretical receiver function

The broadband Green's function method has a rigorous basis in theoretical and computational seismology (Helmberger, 1983), and uses the elastodynamic representation theorem and Green's functions. The earthquake source is represented as a shear dislocation on an extended fault plane, whose radiation pattern, and its tendency to become subdued at periods shorter than about 0.5 sec, are accurately represented. Wave propagation is represented rigorously by Green's functions computed for the seismic velocity structure which contains the fault and the site, or by empirical Green's functions derived from strong motion recordings of small earthquakes. These Green's functions contain both body waves and surface waves. The ground motion time history is calculated in the time domain using the elastodynamic representation theorem. This involves integration over the fault surface of the convolution of the slip time function on the fault with the Green's function for the appropriate depth and distance.

To simulate broadband time histories, the ground motions are computed separately in the short period and long period ranges, and then combined into a single broadband time history (Somerville et al., 1996). The use of different methods in these two period ranges is necessitated by the observation that ground motions have fundamentally different characteristics in these two period ranges. At long periods (longer than about 1 second), strong ground motions are deterministic in the sense that seismological models are capable of matching not only the spectral amplitudes but also the

waveforms of recorded long period ground motions, once the rupture model of the earthquake and the seismic velocity structure of the region surrounding the earthquake are known. At short periods (shorter than about 1 second), strong ground motions become increasingly stochastic in nature. Seismological models are generally capable of matching the spectral amplitudes of the short period ground motions, but are generally not capable of matching the recorded waveforms. The transition from deterministic to stochastic behavior appears to be due to a transition from coherent source radiation and wave propagation conditions at long periods (over long dimensions) to incoherent source radiation and wave propagation conditions at short periods (over short dimensions).

An example of broadband simulation of strong ground motions is shown in Figure 1, which compares the recorded and simulated ground motions at Arleta from the 1994 Northridge earthquake. The broadband nature of the simulation is demonstrated by comparing the recorded and simulated acceleration, velocity and displacement time histories. When compared to observed records of actual earthquakes, such ground motion simulation procedures can reproduce the duration, peak accelerations, and short period (less than 1 sec.) response spectral accelerations within a factor of about 1.5, which is comparable to the uncertainty in empirical ground motion prediction models. For peak velocities and response spectral accelerations at periods longer than 1 sec, the error in prediction by these simulation methods may be lower than that of empirical ground motion models, especially if rupture directivity and basin response affect the data and are included in the predictions. This kind of validation against recorded data constitutes an important criterion for the selection of ground motion simulation procedures for use in earthquake engineering.

Once it has been demonstrated that these seismologically-based ground motion models can take account of specific source, path and site conditions that are of interest, they can then be used to generate ground motion time histories which augment the recorded data used to generate empirical models, or alternatively as site-specific estimates that complement estimates based on empirical models. Through the use of these seismological models of strong ground motion, the number of parameters used in the estimation of strong ground motion has grown beyond the simple set of magnitude, distance and site category. For example, in recent ground motion models, the source and path parameters allow for differences in the ground motions between the hanging wall and foot wall of dipping faults, and for the spatial variations in ground motions around faults due to rupture directivity effects. In place of using simple monotonic models for the attenuation of ground motion with distance, more complex models that take account of seismic wave propagation in a layered crust have been developed. In place of simple geological descriptors of site conditions or ranges of seismic velocity, the complexity of the interaction of waves arriving at the site with the strongly heterogeneous conditions that characterize the shallow geology of most sites has been recognized and analyzed.

Seismological methods are being increasingly used to constrain those aspects of ground motion attenuation relations that are poorly constrained by recorded strong motion data. For example, even in California, there are few strong motion recordings close to the large earthquakes (within 10 km of magnitude 7 and larger events) that control the seismic design of most structures. The reliability of empirical ground motion attenuation models can be enhanced by augmenting the strong motion data base with strong ground motion time histories simulated for these conditions. As we show in the next section, models of ground motion attenuation in eastern North America are based almost entirely on seismological models due to the sparsity of recorded data.

GROUND MOTION ATTENUATION IN EASTERN CANADA

Seismological methods are widely used in ground motion attenuation relations in stable continental regions where recorded strong motion data are sparse. Using the known source characteristics of earthquakes in stable continental regions, and known crustal velocity structure models, we can generate ground motion attenuation models, and examine the influence of earthquake source characteristics and crustal structure on ground motion attenuation in stable continental interiors. We begin with a review of the source characteristics of earthquakes in eastern Canada. We then proceed to describe how crustal velocity structure models influence ground motion attenuation, and how these models can be used in conjunction with earthquake source models to generate ground motion attenuation relations. The application of these seismological models to understanding the characteristics of ground motion attenuation in eastern Canada are then discussed.

Earthquake Source Models for Eastern Canada

Somerville et al. (1987) obtained relationships between seismic moment and source duration, which provide indirect relationships between seismic moment and fault rupture area, for earthquakes in eastern North America and other stable continental interiors. These models indicate a constant stress drop scaling relation with a stress drop of about 120 bars. For the larger magnitudes, the rupture areas of earthquakes in stable continental interiors are smaller than those in tectonically active regions. The resulting higher stress drop is expected to produce larger ground motions. However, in order to predict strong ground motions, we need to characterise not only the overall rupture dimensions, but also detailed aspects of the fault rupture.

Detailed studies of the spatial distribution of slip on the fault plane for 15 crustal earthquakes in tectonically active regions, derived from strong motion recordings and other data, have shown that the slip distribution is highly variable, characterized by asperities (regions of large slip) surrounded by regions of low slip. These slip models have been used to develop relationships between seismic moment and a set of fault parameters that are needed for predicting strong ground motions (Somerville et al., 1999). These parameters include fault length, fault width, rise time (duration of slip at a point on the fault), and the size, slip contrast and location of asperities. Hartzell et al. (1994) obtained detailed models of the distribution of slip on the fault for three earthquakes in eastern Canada: the 1983 Miramichi, 1988 Saguenay and 1989 Ungava earthquakes. The slip models of these three earthquakes are characterized by strong spatial variation in slip over the fault surface (Figure 2), like those of earthquakes in tectonically active regions. The smaller rupture areas and longer rise times of these three earthquakes compared with those of 15 crustal earthquakes in tectonically active regions are evident in Figure 3. The longer rise times result from the larger average displacement over a smaller fault area. The smaller fault area for a given earthquake magnitude is expected to give rise to stronger ground motion amplitudes.

The depth range of faulting is an important issue in the source characterization of earthquakes in stable continental interiors. There is direct surface evidence that shallow faulting occurred in hard rock in several earthquakes in Australia. Also, seismogenic faulting at shallow depths is inferred to have occurred during the Ungava, Quebec earthquake (Figure 2), and the 1978 Meckering, Australia earthquake based on the analysis of teleseismic data (Langston, 1987). It has been proposed (Marone and Scholz, 1988) that the top of the seismogenic zone is controlled by a transition from brittle to ductile behaviour due to the presence of unconsolidated fault gouge. They hypothesize that this causes the cutoff of seismicity that is observed in well developed fault zones at depths shallower than 3-5 km. This cutoff in seismicity is correlated with relatively low seismogenic slip (low stress drop) at shallow depth that is characteristic of slip models of earthquakes in tectonically active regions inferred from strong motion data. The cutoff in seismicity at shallow depth is not observed on faults which are poorly developed, such as in the 1978 Meckering, Australia and the 1983 Miramichi, New Brunswick earthquakes, where seismicity extends up to the surface.

In tectonically active regions, it is commonly assumed that the zone of the fault that contributes significantly to seismic radiation is confined to depths where there exist crystalline rocks, even when there is surface fault rupture, and the seismogenic depth is typically assumed to be several km. This assumption is probably invalid in stable continental interiors. Strong motion simulations incorporating shallow seismogenic faulting have very large ground motions at close distances if it is assumed that the rise time of slip on the fault is uniform over the fault rupture. However, faulting in the Ungava earthquake, which was confined to the upper 2 km (Figure 2), was accompanied by an unusually long rise time (Figure 3), which would reduce the level of ground motions close to shallow faulting.

Crustal Waveguide Effects

The fundamental nature and consequent predictive capability of the broadband Green's function approach was demonstrated at an early stage in the development of ground motion attenuation relations for stable continental interiors. Burger et al. (1987) used simple wave propagation calculations in a horizontally layered crust to explain a flattening in the rate of attenuation that was observed in recordings of small earthquakes in the central and eastern United States (Figure 4a). The following year, the effect of crustal structure on the attenuation of ground motion was more clearly demonstrated in the strong motion recordings of the 1988 Saguenay, Quebec earthquake, as shown in Figure 5 (Somerville et al., 1990).

At close distances (within about 50 km), the largest ground motions are caused by waves that travel upward from the earthquake source to the site (Figure 4a). However, as distance from the source increases, the direct wave becomes

weaker, and the reflections of downgoing waves from interfaces below the source reach the critical angle and undergo total internal reflection. The strong contrast in elastic moduli at these interfaces, especially the Moho, causes these critical reflections to have large amplitudes. The arrival of these critical reflections, beginning at a distance of about 50 km, causes a reduction in the rate of attenuation of ground motion out to distances of about 100 km or more. While the elevated ground motion amplitudes in this distance range are usually not large enough by themselves to cause damage, they may produce damage if combined with the amplifying effects of soft soils. The destructive potential of these effects was dramatically demonstrated in the 1989 Loma Prieta earthquake (Somerville et al., 1994), in which major damage was done to buildings and bridges in the San Francisco Bay area located 80 to 90 km from the earthquake.

The degree of reduction in rate of attenuation relation caused by the crustal waveguide, and the distance range over which it occurs, depend on the depth of the earthquake and the thickness and velocity profile of the crust. Consequently, ground motion attenuation characteristics vary depending on the crustal structure and the depth of the earthquake. This new understanding of ground motion attenuation relations has had a large impact on ground motion attenuation relations, especially in regions such as eastern North America where the main basis for attenuation relations is provided by seismologically based models. Whereas earlier seismological models used simple half-space approximations for the attenuation of ground motion (1/R for body waves at close distances; $1/(R)^{1/2}$ for surface waves at larger distances, where R is distance), all of the current models now take account of the effect of the crustal waveguide. Some methods do so by using attenuation functions derived from recorded weak motion data (e.g. from regional and national earthquake networks; Atkinson and Boore, 1995; 1997), while others use wave propagation calculations based on the regional crustal structure and the earthquake depth (Saikia et al., 1998).

The broadband Green's function procedure has been tested against ground motion data recorded on the broadband digital stations of the National Seismic Network in the central and eastern United States. Using a crustal model derived from the data, synthetic seismograms were generated and their peak velocities were compared with those of recorded data. A basic feature of the empirical attenuation data, shown by the circles in Figure 4b, is a decrease in the rate of attenuation centered at a distance of about 100 km, and typically extending from about 75 km to several hundred km, due to critical reflections from the lower crust. Using a crustal velocity model derived from the NSN data, we were able to match the shape of the empirical attenuation using synthetic seismograms, whose median amplitude is shown by the thick irregular line in Figure 4b.

The sensitivity of the attenuation relation to various source parameters was analyzed using synthetic seismograms. The attenuation at close distances, in the region of the first shoulder in Figure 4b, is strongly dependent on the focal depth of the earthquake. At distances larger than about 30 km, the shape of the attenuation is less sensitive to the focal depth, except for shallow earthquakes for which trapping of energy in the shallow low velocity region causes gradual attenuation. Also, for deeper earthquakes, there is some influence because changes in focal depth cause changes in the critical distance for reflected phases from the lower crust. The sensitivity of ground motion amplitudes to changes in the anelastic attenuation of the crust only becomes significant at distances larger than about 75 km.

Based on the empirical model and synthetic seismograms, an attenuation model (shown by the smooth lines in Figure 4b) that includes two shoulders (regions of steep slope) was developed. The first shoulder occurs within a few tens of km from the source, and the second shoulder occurs at several hundred km from the source. The two shoulders are separated by an interval of more gradual attenuation. The second shoulder is well constrained by the recorded data and by the synthetic seismograms. Although the recorded data were insufficient to constrain the first shoulder, the values calculated from synthetic seismograms, which overlap the recorded data at distances larger than 100 km, were used to extrapolate to closer distances and define the first shoulder.

In summary, seismological methods are needed for developing ground motion attenuation relations in stable continental regions where recorded strong motion data are sparse. Using the known source characteristics of earthquakes in stable continental regions, and known crustal velocity structure models, we can generate ground motion attenuation models, and examine the influence of earthquake source characteristics and crustal structure on ground motion attenuation in stable continental interiors.

EFFECTS OF SEDIMENTARY BASINS ON STRONG GROUND MOTIONS

Many urban regions, including Vancouver, are situated on deep sediment-filled basins. A basin consists of alluvial deposits and sedimentary rocks that are geologically younger and have lower seismic wave velocities than the underlying rocks upon which they have been deposited. Basins have thicknesses ranging from a hundred meters to over ten kilometers. Waves that become trapped in deep sedimentary basins can potentially be very damaging. Basin effects caused widespread damage in Caracas during the 1977 Caracas earthquake; in Mexico City during the 1985 Michoacan earthquake; and in Santa Monica and West Los Angeles during the 1994 Northridge earthquake.

Conventional criteria for characterizing site response are typically based on the distribution of shear wave velocity with depth in the upper 30 meters as determined from field measurements. The response of this soil layer is usually modeled assuming horizontal layering, following the method illustrated on the left side of Figure 6. The wave that enters the layer may resonate in the layer but cannot become trapped within the layer.

However, at periods longer than one second, seismic waves have wavelengths that are much longer than 30 meters, and their amplitudes are controlled by geological structure having depths of hundreds or thousands of meters which in many cases, like that of sedimentary basins, is not horizontally layered. If the wave enters a basin through its edge, it can become trapped within the basin if post-critical incidence angles develop. The resulting total internal reflection at the base of the layer is illustrated at the top right of Figure 6. In the lower part of Figure 6, simple calculations of the basin response are compared with those for the simple horizontal layered model. In each case, a plane wave is incident at an inclined angle from below. The left side of the figure shows the amplification due to impedance contrast effects that occurs on a flat soil layer overlying rock (bottom) relative to the rock response (top). A similar amplification effect is shown for the basin case on the right side of the figure. However, in addition to this amplification, the body wave entering the edge of the basin becomes trapped, generating a surface wave that propagates across the basin. Current empirical ground motion attenuation relations do not distinguish between sites located on shallow alluvium and those in deep sedimentary basins, and tend to underestimate the ground motions recorded in basins.

Comparing strong ground motion measurements with the results of computer simulations has substantially increased our understanding of basin effects. For example, Figure 7 shows strong motion velocity time histories of the 1994 Northridge earthquake recorded on a profile of stations that begins in the San Fernando Valley, crosses the Santa Monica mountains and extends into the Los Angeles basin (Graves et al., 1998). The two dashed lines indicate the arrival of shear waves from the two predominant subevents of the earthquake. The time histories recorded on rock sites in the Santa Monica Mountains are brief, and are dominated by the direct waves. In contrast, the time histories recorded in the Los Angeles basin have long durations, and the peak velocities are associated not with the direct waves but from later arriving waves that are known to be waves generated at the northern edge of the Los Angeles basin (bottom right of Figure 7). Much of the damage in the Los Angeles basin during the Northridge earthquake, including the collapse of the I10 freeway and damage to numerous large buildings in Santa Monica and West Los Angeles, may be attributable to basin effects.

Basin Edge Effects

The largest basin effect in the Los Angeles basin during the Northridge earthquake occurred just south of the Santa Monica fault. In this region, the basin-edge geology is controlled by the active strand of the westward striking Santa Monica fault, shown in map view and cross section in the upper part of Figure 7. Despite having similar surface geology, sites to the north of the fault show relatively modest amplitudes, whereas sites to the south of the fault exhibit significantly larger amplitudes, with a clear and immediate increase in amplification occurring at the fault scarp. The same pattern is dramatically reflected in the damage distribution indicated by red tagged buildings at the top of Figure 7, which shows a large concentration of damage immediately south of the fault scarp in Santa Monica. The strong correlation of ground motion amplification pattern with the fault location suggests that the underlying basin-edge geology is controlling the ground motion response. This is confirmed in the 2D synthetic seismograms shown in Figure 7. The large amplification results from constructive interference of direct waves with the basin-edge generated surface waves.

The 1995 Kobe earthquake provided further evidence from recorded strong motion data, supported by wave propagation modeling using basin edge structures, that ground motions may be particularly large at the edges of fault-controlled basins. Severe damage to buildings due to the Kobe earthquake was observed in a zone about 30 km long and

1 km wide, and offset about 1 km southeast of the fault on which the earthquake occurred (Figure 8). The near-fault ground motions generated by rupture directivity effects (discussed further below) in the Kobe earthquake were further amplified by the basin edge effect. This effect was caused by the constructive interference between direct seismic waves that propagated vertically upward through the basin sediments from below, and seismic waves that diffracted at the basin edge and proceeded laterally into the basin (Kawase, 1996; Pitarka et al., 1998). The basin edge effect caused a concentration of damage in a narrow zone running parallel to the faults through Kobe and adjacent cities (Figure 8). The observed band of damage, represented by the zone of JMA Intensity VII shown in panel (a), is reproduced in the map of simulated peak velocity (panel c), generated using a 3D model of the basin edge (panel b). The strong influence of the basin edge is demonstrated in the lower part of the figure (panel d), which shows vertically aligned time histories from 2D simulations for the actual basin geometry (left side) and a flat layered model with no basin edge (right side). The basin structure produces a strongly asymmetrical zone of large amplitudes along the edge of the basin.

Focusing Effects

The damage pattern caused by the Northridge earthquake was characterized by pockets of localized damage such as those in Sherman Oaks and Santa Monica that were not clearly correlated with surficial soil conditions (Hartzell et al., 1997). These observations have produced important new insights into the causes of localized zones of damage. During the Northridge earthquake, deeper lying geological structure may have had as much influence on strong motion patterns as the upper 30 meters that are conventionally used to characterize site response. This deeper structure may include sedimentary structures in the upper few kilometers of sedimentary basis, as well as topography on the underlying sediment/basement interface. These structures, in the form of folds and buried basins, focus energy (like a lens) in spatially restricted areas on the surface, in some cases becoming the dominant factor in the modification of local ground motion amplitudes.

NEAR-FAULT GROUND MOTIONS

The distribution of ground motion amplitudes in the near-fault region is strongly influenced by the fault geometry. For vertical strike-slip faults, rupture directivity effects cause a strong spatial variation in ground motions for a given closest distance to the fault. For dipping faults, there are two prominent effects: the rupture directivity effect and the hanging wall effect. The hanging wall effect is due mainly to the proximity of much of the fault to hanging wall sites. It is most pronounced for periods shorter than about 1 second, and occurs away from the top edge of the fault on the hanging wall side. The rupture directivity effect is due to rupture propagation and radiation pattern effects. It is most pronounced at periods longer than 1 second, and is concentrated over the top edge of the fault. The relationship between the rupture directivity effect and the hanging wall effect is thus complementary both spatially and in period range, enhancing the degree of spatial variation of strong ground motion around dipping faults. In the following, we describe empirical models that have been developed to represent these spatial variations.

Hanging Wall Effects

Sites on the hanging wall of a dipping fault have closer proximity to the fault as a whole than do sites at the same closest distance on the foot wall. This causes larger short period ground motions on the hanging wall than on the foot wall at the same closest distance. Abrahamson and Somerville (1996) compared the ground motions for sites on the hanging wall with those on the foot wall and those off the end of the fault rupture. They found a significant systematic increase in ground motions for sites over the hanging wall, but the decrease in ground motions for sites on the foot wall was not as systematic. Accordingly, the ground motions from dipping faults were divided into two categories: sites on the hanging wall side of the rupture and within the edge of the rupture, and sites on the foot wall or off the end of the rupture. The effect is greatest (a factor of 1.45) in the closest distance range of 8 to 18 km, and is significant (larger than a factor of 1.2) in the distance range of 6 to 22 km for periods between 0 to 0.6 seconds. The maximum hanging wall effect is a factor of 1.45 in the period range of 0 to 0.6 seconds, decreasing to unity at 5 seconds. In the distance range of 8 to 18 km, the effect is significant in the period range of 0 to 1.8 seconds. This model of hanging wall effects was incorporated into the ground motion model of Abrahamson and Silva (1997).

Near-Fault Rupture Directivity Effects

The propagation of fault rupture toward a site at a velocity that is almost as large as the shear wave velocity causes most of the seismic energy from the rupture to arrive coherently in a single large long period pulse of motion which occurs at the beginning of the record. This pulse of motion represents the cumulative effect of most of the seismic radiation from the fault. The radiation pattern of the shear dislocation on the fault causes this large pulse of motion to be oriented in the direction perpendicular to the fault, causing the strike-normal peak velocity to be larger than the strike-parallel peak velocity. The enormous destructive potential of near-fault ground motions was manifested in the 1994 Northridge and 1995 Kobe earthquakes. In each of these earthquakes, peak ground velocities as high as 175 cm/sec were recorded (Figure 9). The period of the near-fault pulses recorded in both of these earthquakes lie in the range of 1 to 2 seconds, comparable to the natural periods of structures such as bridges and mid-rise buildings, many of which were severely damaged.

Near-fault rupture directivity effects were first observed in the strong ground motions recorded during the 1966 Parkfield earthquake, and practically all subsequent earthquakes recorded in California showed clear evidence of these effects. However, although the nature of near-fault rupture directivity effects was soon clearly identified, ground motion models that explicitly account for these effects have only been developed during the past few years. Based on an empirical analysis of near-fault data, Somerville et al. (1997) developed modifications to empirical strong ground motion attenuation relations to account for the effects of rupture directivity on strong motion amplitudes and durations. In order to best represent near-fault ground motions in engineering design, the differences between ground motions in the directions normal to and parallel to the fault strike may need to be taken into account. The design and evaluation of critical structures located near faults often uses time histories containing near-fault pulses whose response spectra are compatible with a design response spectrum. However, the response spectrum is not capable of adequately describing the seismic demands presented by brief, impulsive near-fault ground motions. This indicates the need to use time domain parameters of the near-fault pulse, such as the period and amplitude of the directivity pulse, in conjunction with the response spectrum, as parameters for specifying near-fault ground motion characteristics for design. These pulse parameters are controlled by source parameters such as the rise time of slip on the fault (Figure 3b).

URBAN GROUND MOTION MAPPING

In the preceding sections, we have described several ground motion effects related to various source, path and site characteristics that can affect the ground motions at a site. The challenge of urban hazard mapping is to predict these effects not just at a single site but over an extended region, and to do so with an acceptable level of reliability. The difficulty of this challenge is manifested in the spatially irregular patterns of damage that are observed after major earthquakes.

Historically, ground motion maps of past earthquakes have used intensity as the ground motion parameter, because there have not been enough ground motion recordings to make reliable maps of instrumental ground motion parameters, and ground motion simulation procedures have not been sufficiently developed. However, these conditions are now changing. For example, the HAZUS Loss Estimation Methodology developed by FEMA in the United States is based on instrumental ground motion parameters, not intensity. This has required the development of instrumental ground motion maps of past earthquakes for use in calibrating loss estimation methodologies. Ground motion maps of earthquakes such as the 1989 Loma Prieta and Northridge events, generated for the calibration of HAZUS (Pitarka et al., 1996; Somerville et al., 1995), demonstrate that strong motion recording stations in some major urban regions may now be sufficiently dense to provide a first order estimate of the distribution of ground motions. However, they are not dense enough to map local variations in ground motions, or provide direct evidence on the correlation of local damage patterns with spatial variations in ground motion levels. Computational methods for seismic zonation can potentially be used to interpolate the recorded data to give a more detailed map of local variations, provided that the subsurface structure is adequately characterized. These methods will need to be validated by the deployment of very dense strong motion networks in selected urban regions.

The conventional approach to zonation of ground shaking hazards in urban regions is to assume that the geology can be characterized by a horizontally stratified medium, and that only the shallowest few tens of meters influence the ground motion characteristics. Seismic zonation then consists of linking together site-by-site estimates of site response generated

using methods such as that shown on the left hand side of Figure 6. However, as demonstrated on the right hand side of Figure 6 and illustrated in Figures 7 and 8, this simple approach may significantly underestimate the amplitudes and durations of strong ground motions, especially at periods of about one second and longer, that can become trapped within sedimentary basins due to critical reflections that are set up at the edges of the basin. These effects are due to the geometry of the interface between the sedimentary materials and the underlying crystalline rocks, and cannot be explained by the shallow soil profile alone. Many elements of the urban infrastructure, such as bridges, multi-story buildings, dams and storage tanks, are susceptible to long-period ground motions which may be influenced by basin effects.

New computational procedures have the potential for greatly enhancing the reliability of seismic zonation of urban regions located in sedimentary basins. It is expected that wave propagation computations using finite difference and other methods will largely supplant the use of simple 1-D models of site response in urban seismic zonation. The rapid increase in the speed and memory of computers, and the development of efficient computational methods for modeling seismic wave propagation in laterally varying geological structure, enable us to model the effects of sedimentary basins on ground motions generated by scenario earthquakes. By using finite difference techniques (Graves, 1993), we are able to compute the complete wave field up to a given frequency threshold throughout an entire urban region. This capability has the potential to greatly enhance the seismic zonation of urban regions located on sedimentary basins. Instead of obtaining ground motion estimates at a set of discrete locations using local flat layered geological models, which may be inaccurate because they do not account for the effects of the basin structure, we are able to calculate the seismic wave field throughout the urban region, with the ground motion characteristics at each location reflecting the effects of the laterally varying geologic structure in its vicinity.

CONCLUSIONS

In most empirical ground motion attenuation relations, ground motion parameters are predicted using a simplified model in which the effects of the earthquake source are represented by earthquake magnitude; the effects of wave propagation from the earthquake source to the site region are specified by a distance; and the effects of the site are specified by a site category. These ground motion models have a large degree of uncertainty because other conditions that are known to have an important influence on strong ground motions, such as near-fault rupture directivity effects and basin response effects, are not treated as parameters of these simple models. In order to reduce the uncertainty in ground motion prediction at a given site, we need to augment the parameterization of ground motion models to include more realistic representations of source, path and site effects. Seismological models are being increasingly used to constrain those aspects of ground motion attenuation relations that are poorly constrained by recorded strong motion data.

Ground motion maps of future scenario earthquakes have played an important role in urban planning and mitigation activities. To date, these ground motion maps have used simplified procedures. However, there are many ground motion effects, such as those described above, that have typically not been addressed. These include source effects such as those due to rupture directivity or the orientation of the fault (hanging wall effect), and the effects of deep structure such as sedimentary basins, basin edges, and buried folds and faults. Development of procedures to take account of these effects will ultimately make earthquake scenario maps and seismic zonation more tractable, but will increase the complexity of their production.

REFERENCES

Abrahamson, N.A. and K. Shedlock (1997). Overview, ground motion attenuation relations, *Seismological Research Letters* 68, 9-23.

Abrahamson, N.A. and W.J. Silva (1997). Empirical response spectral attenuation relations for shallow crustal earthquakes, *Seismological Research Letters* 68, 94-127.

Abrahamson, N.A. and P.G. Somerville (1996). Effects of the hanging wall and footwall on ground motions recorded during the Northridge Earthquake, *Bull. Seism. Soc. Am.*, 86, S93-S99.

Abrahamson, N.A. and R.R. Youngs (1992). A stable algorithm for regression analysis using the random effects model. *Bull. Seism. Soc. Am.* 82, 505-510.

Atkinson, G. and D. Boore (1997). Some comparisons between recent ground motion relations, *Seism. Res. Lett.* 68, 24-40.

Atkinson, G. and D. Boore (1995). New ground motion relations for eastern North America, *Bull. Seism. Soc. Am.* 85, 17-30.

Atkinson, G. (1993). Source spectra for earthquakes in eastern North America. *Bull. Seism. Soc. Am.* 83, 1778-1798.

Boatwright, J. and G. Choy (1992). Aceleration source spectra anticipated for large earthquakes in eastern North America, *Bull. Seism. Soc. Am.*, 82, 660-682.

Boore, D.M. (1983). Stochastic simulation of high-frequency ground motions based on seismological models of the radiated spectra. *Bull. Seism. Soc. Am.* 73, 1865-1894.

Burger, R.W., P.G. Somerville, J.S. Barker, R.B. Herrmann, and D.V. Helmberger (1987). The effect of crustal structure on strong ground motion attenuation relations in eastern North America, *Bull. Seism. Soc. Am.*, **77**, 420-439

Electric Power Research Institute (1993). Guidelines for determining design basis ground motions. EPRI TR-102293.

Graves, R.W., A. Pitarka and P.G. Somerville (1998). Ground motion amplification in the Santa Monica Area: Effects of shallow basin edge structure, *Bull. Seism. Soc. Am.*, 88, 1224-1242.

Graves, R. W. (1966). Simulating seismic wave propagation in 3D elastic media using staggered-grid finite-differences, *Bull. Seism. Soc. Am.*, 86, 1091-1106.

Graves, R.W. (1993). Modeling three-dimensional site response effects in the Marina District Basin, San Francisco, California. *Bull. Seism. Soc. Am.*, 83, 1042-1063.

Hartzell, S., E. Cranswick, A. Frankel, D. Carver and M. Meremonte (1997). Variability of Site Response in the Los Angeles Urban Area, *Bull. Seism. Soc. Am.*, 1377-1400.

Hartzell, S., C. Langer and C. Mendoza (1994). Rupture histories of eastern North American earthquakes. *Bull. Seism. Soc. Am.* 84, 1703-1724.

Helmberger, D.V. (1983). Theory and application of synthetic seismograms, in Earthquakes: Observation, Theory and Interpretation, Proc. Int. Sch. Phys. "Enrico Fermi" Course LXXXV, pp. 174-221, eds. Kanamori, H. and E. Boschi, North-Holland, Amsterdam.

Langston, C.A. (1987). Depth of faulting during the 1968 Meckering, Australia earthquake sequence determined from waveform analysis of local seismograms, *J. Geophys. Res., 87,* 11561-11574.

Marone, C. and C.H. Scholz (1988). The depth of seismic faulting and the upper transition from stable to unstable slip regimes, *Geophys. Res. Lett.* 15, 621-624.

Kawase, H. (1996). The cause of the damage belt in Kobe: "The Basin-Edge Effect," constructive interference of the direct S-wave with the basin-induced diffracted/Rayleigh waves, Seismological Research Letters 67, 25-34.

Pitarka, A., K. Irikura, T. Iwata and H. Sekiguchi (1998). Three-dimensional simulation of the near-fault ground motion for the 1995 Hyogo-ken Nanbu (Kobe), Japan, earthquake. *Bull. Seism. Soc. Am.* 88, 428-440.

Pitarka, A., P.G. Somerville and N.F. Smith (1997). Contour maps of ground motions from the 1989 Loma Prieta earthquake. Report prepared for Kircher & Associates.

Saikia, C.K., P.G. Somerville, H.K. Thio, N.F. Smith, A. Pitarka, and B.B. Woods (1998). Crustal structure and ground motion models in the eastern and central United States from National Seismographic Network Data, NUREG/CR-6593, 156 pp.

Somerville, P.G., K. Irikura, R. Graves, S. Sawada, D. Wald, N. Abrahamson, Y. Iwasaki, T. Kagawa, N. Smith and A. Kowada (1999). Characterizing earthquake slip models for the prediction of strong ground motion. *Seismological Research Letters* 70, 59-80.

Somerville, P.G., and T. Sato (1998). Correlation of Rise Time with the Style-of-Faulting Factor in Strong Ground Motions. *Seismological Research Letters* 69, 153.

Somerville, P.G., N.F. Smith, R.W. Graves, and N.A. Abrahamson (1997). Modification of empirical strong ground motion attenuation relations to include the amplitude and duration effects of rupture directivity, *Seismological Research Letters* 68, 199-222.

Somerville, P., C.K. Saikia, D. Wald, and R. Graves (1996). Implications of the Northridge earthquake for strong ground motions from thrust faults, *Bull. Seism. Soc. Am.,* 86, S115- S125.

Somerville, P.G., R.W. Graves, and C.K. Saikia (1995). Characterization of Ground Motions during the Northridge Earthquake of January 17, 1994. *Program to Reduce the Earthquake Hazards of Steel Moment Frame Buildings,* SAC Report 95-03.

Somerville, P.G., N.F. Smith, and R.W. Graves (1994). The effect of critical Moho reflections on the attenuation of strong motion from the 1989 Loma Prieta earthquake, in *"The Loma Prieta, California, Earthquake of October 17, 1989 - Strong Ground Motion,"* U.S. Geological Survey Professional Paper 1551-A, A67-A75. 8, 195-219.

Somerville, P.G., J.P. McLaren, C.K. Saikia, and D.V. Helmberger (1990). The November 25, 1988 Saguenay, Quebec earthquake: source parameters and the attenuation of strong ground motion. *Bull. Seism. Soc. Am.,* 80, 1118-1143.

Somerville, P.G., J.P. McLaren, L.V. LeFevre, R.W. Burger and D.V. Helmberger (1987). Comparison of source scaling relations of eastern and western North American earthquakes, *Bull. Seism. Soc. Am.*, **77**, 332-346.

Toro, G.R., N.A. Abrahamson, and J.F. Schneider (1997). Modeling of strong ground motions from earthquakes in Central and Eastern North America: best estimates and uncertainties. *Seism. Res. Lett.* 68, 41-57.

Youngs, R.R., N.A. Abrahamson, F.I. Makdisi, and K. Sadigh (1995). Magnitude-dependent variance of peak ground acceleration, *Bull. Seism. Soc. Am.* 85, 1,161-1,176.

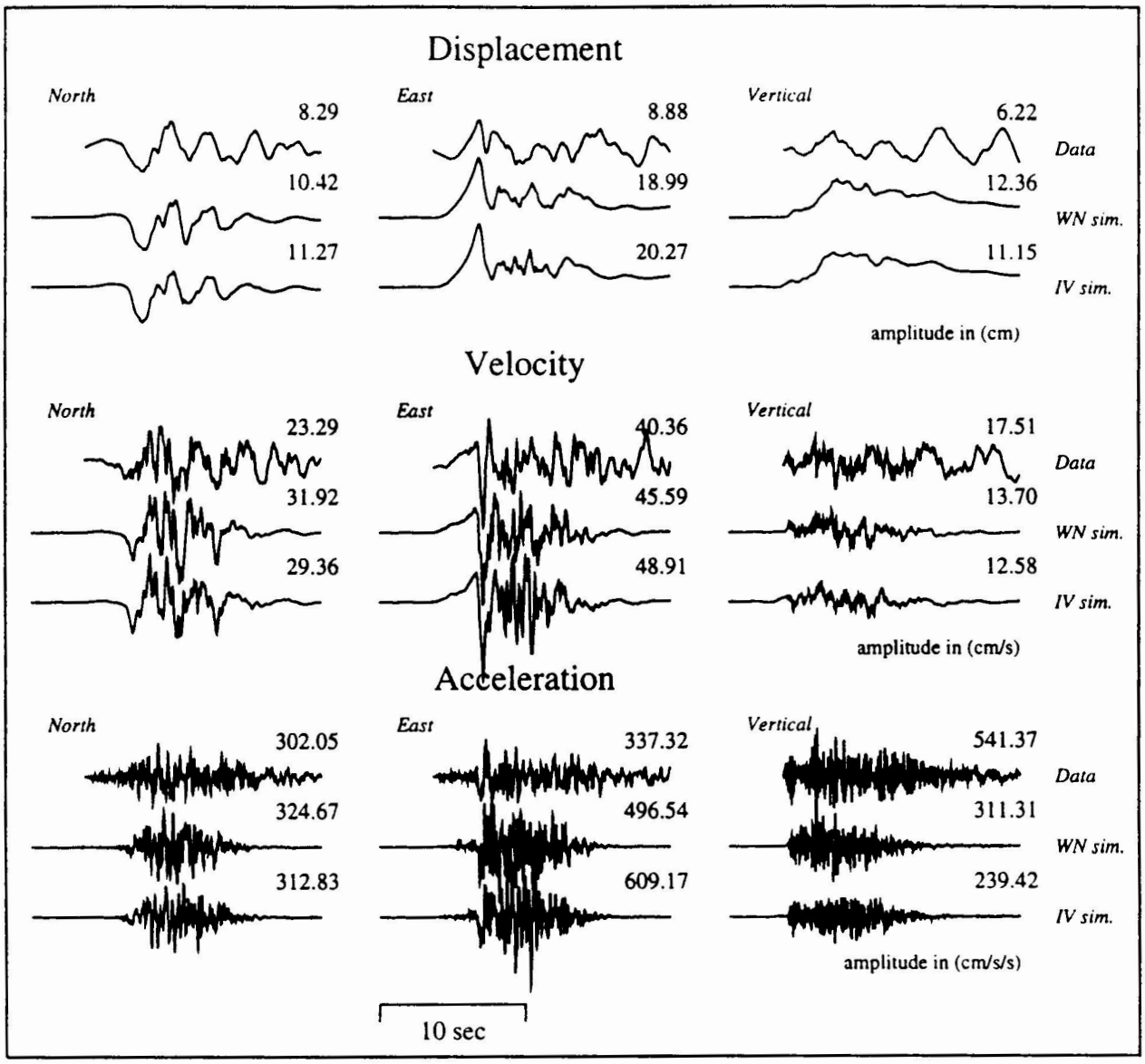

Figure 1. Comparison of recorded (top row) and simulated (middle and bottom rows) displacement, velocity and accelerations at Arleta from the 1994 Northridge earthquake, plotted on a common scale with peak value given at the top left corner. Source: Somerville et al., 1995.

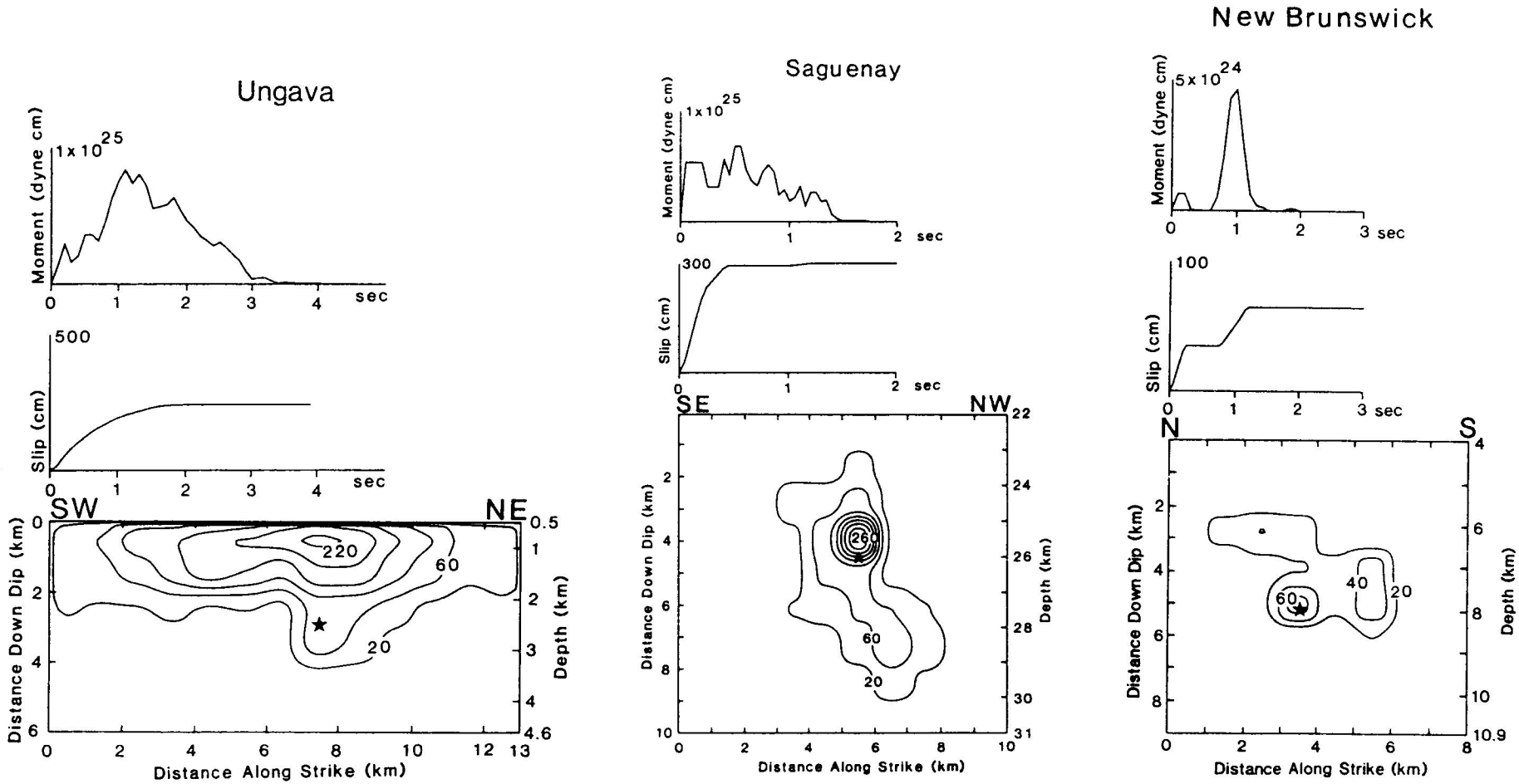

Figure 2. Rupture models of three eastern North American earthquakes. For each event, the bottom panel shows the contours of slip in cm on the fault plane, and the hypocenter is indicated by a star. The middle panel shows the slip function on the fault at its point of maximum slip. The top panel shows the moment rate function. Source: Hartzell et al., 1994.

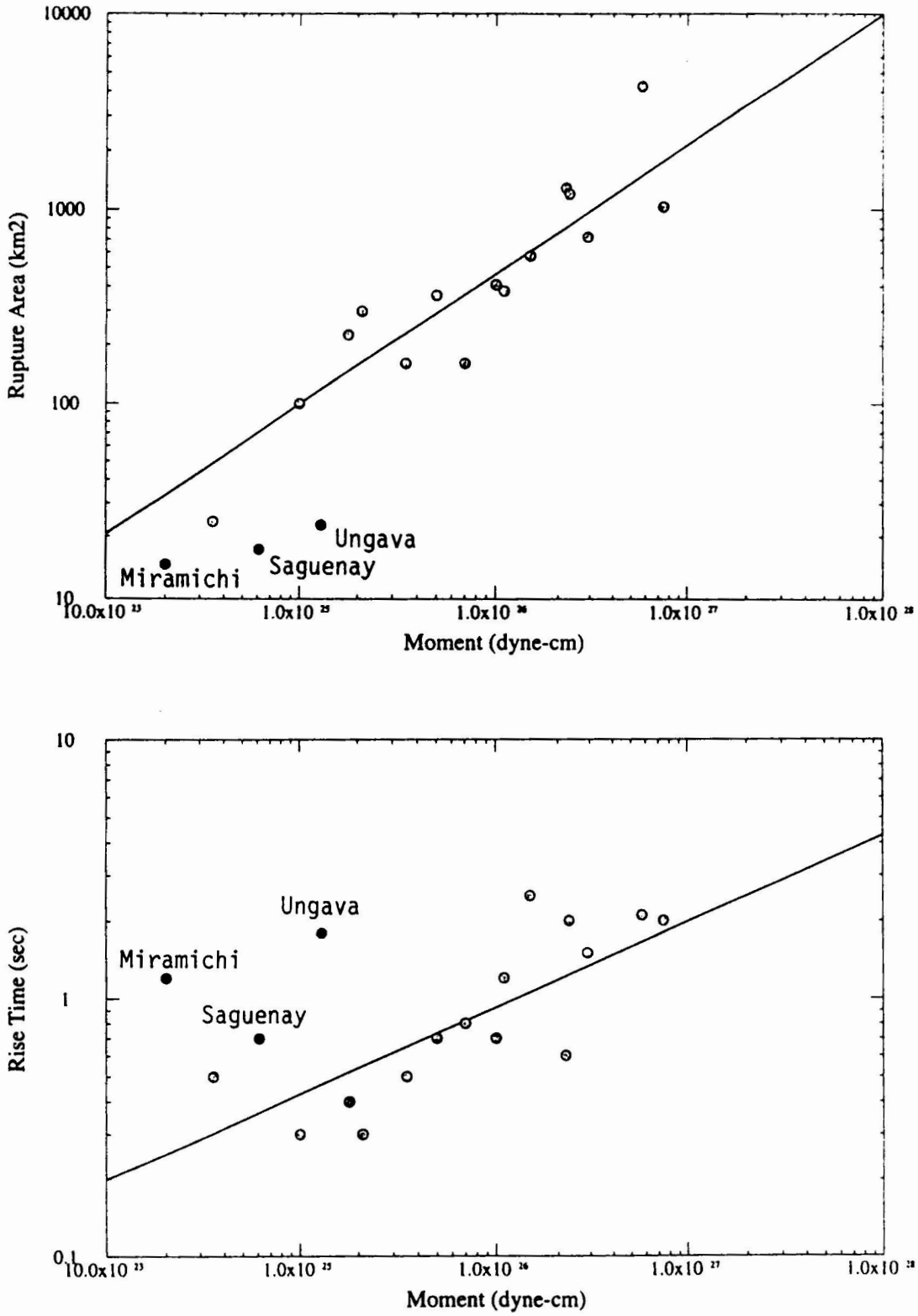

Figure 3. Comparison of fault rupture area (top) and rise time (bottom) of the three eastern Canadian earthquakes in Figure 2 with those of 15 earthquakes in tectonically active areas whose self-similar scaling relations are also shown (Somerville et al., 1999). The three events have smaller rupture areas and hence larger average slip (not shown) and longer rise times that those of earthquakes in tectonically active areas.

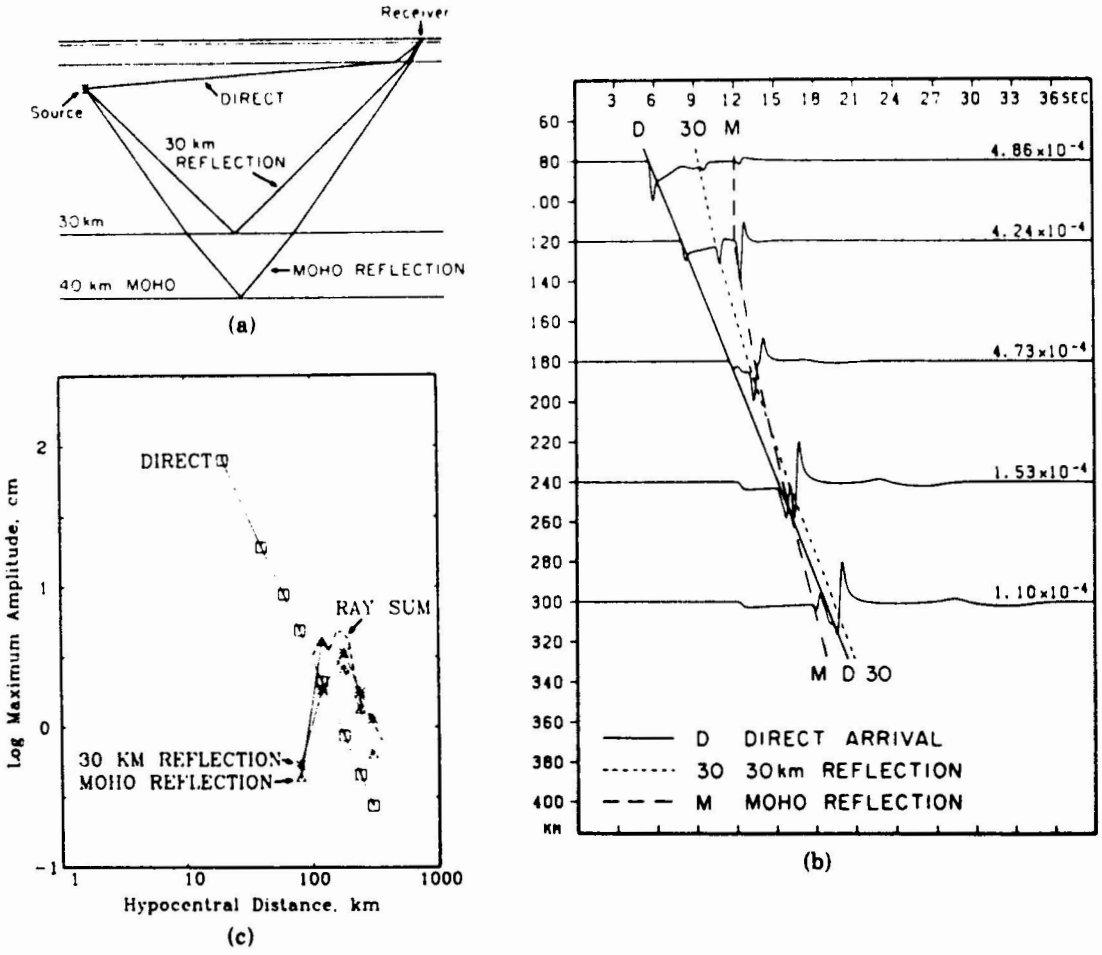

Figure 4a. Effect of crustal structure on ground motion attenuation. Panel (b) shows synthetic seismograms calculated for the crustal waveguide in panel (a), which shows the paths of direct and reflected rays whose contributions to the attenuation relation are shown in Panel (c). Source: Burger et al., 1987.

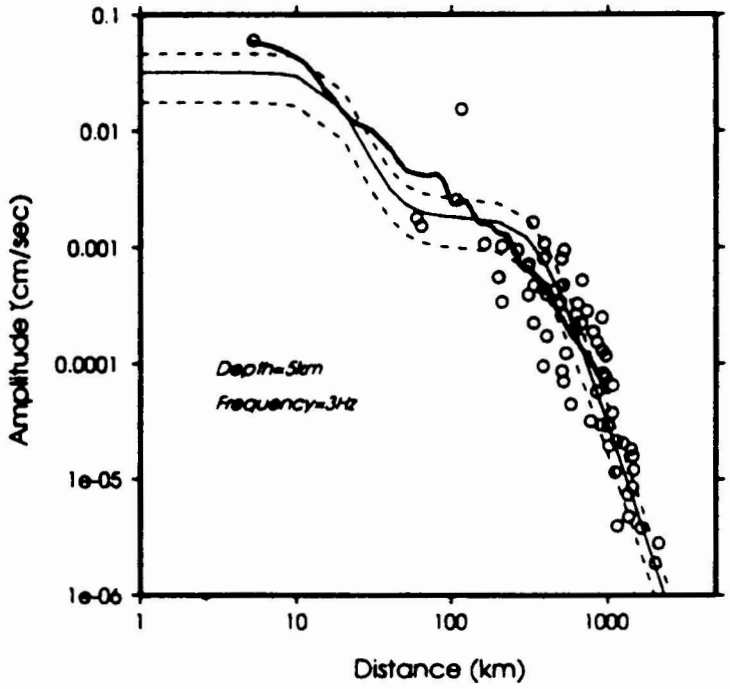

Figure 4b. Recorded spectral velocities at 3 Hz of three earthquakes in the northeastern U.S. (circles); simulated attenuation curve (irregular solid line), and attenuation model (smooth solid and dashed lines). Source: Saikia et al., 1998.

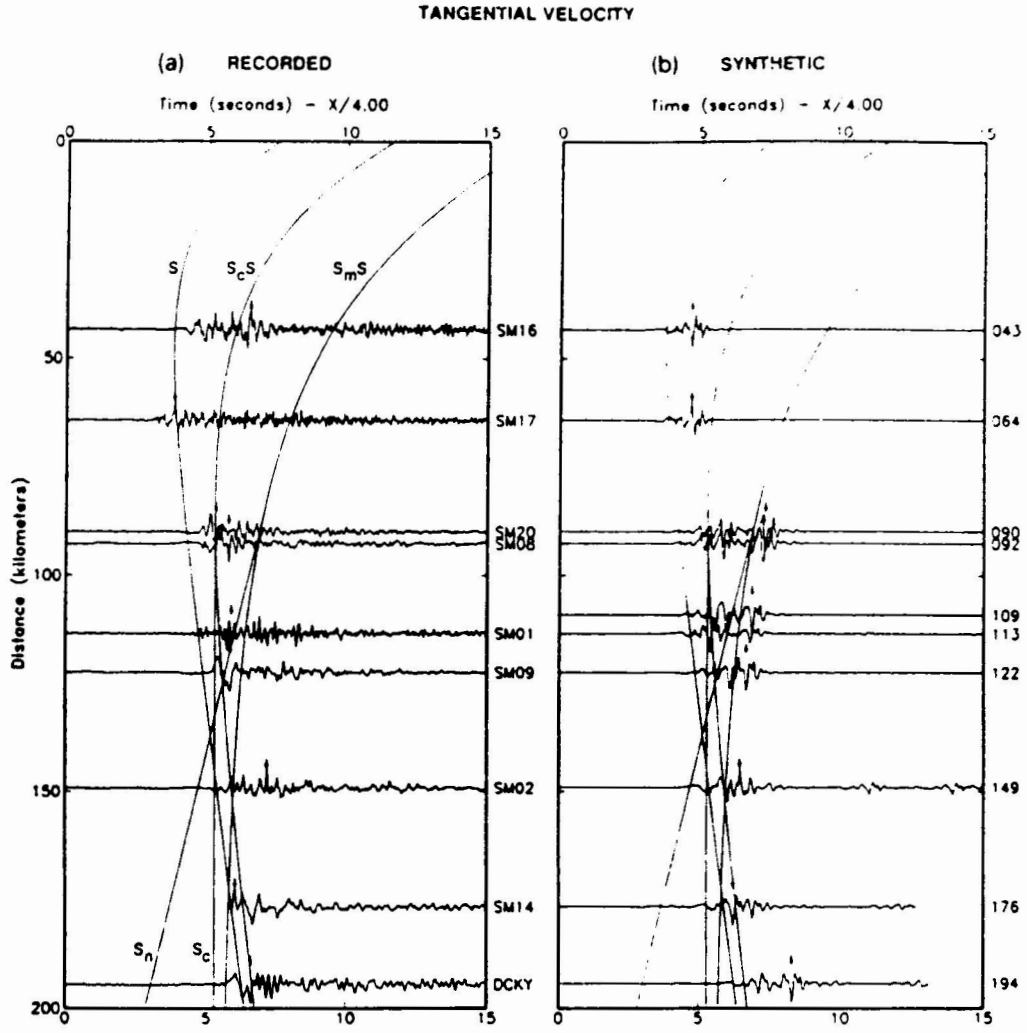

Figure 5a. Profiles of (a) recorded and (b) synthetic ground velocity of the 1988 Saguenay, Quebec earthquake using a travel time reduction of 4.0 km/sec. Seismograms are individually normalized, and the travel time curves are for the direct S, Conrad reflection S_cS, and the Moho reflection S_mS. Source: Somerville et al., 1990.

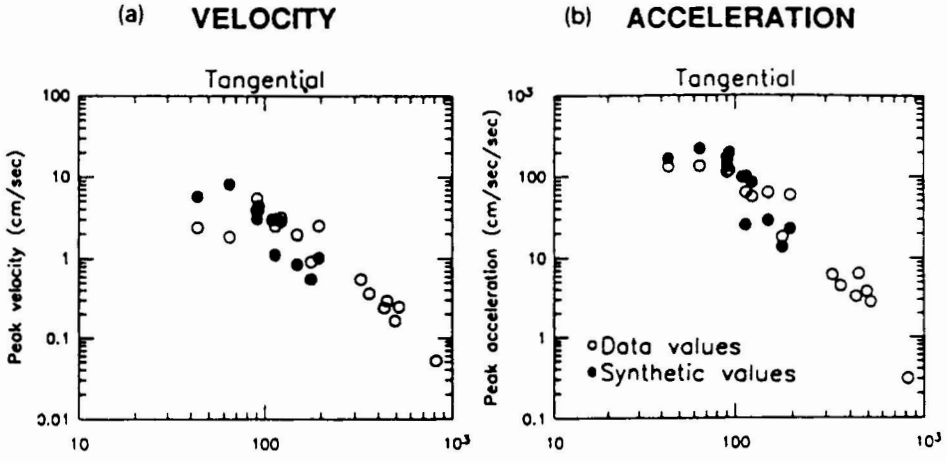

Figure 5b. Attenuation of (a) peak velocity and (b) peak acceleration of the 1988 Saguenay, Quebec earthquake. Circles are recorded values and dots are synthetic values. Source: Somerville et al., 1990.

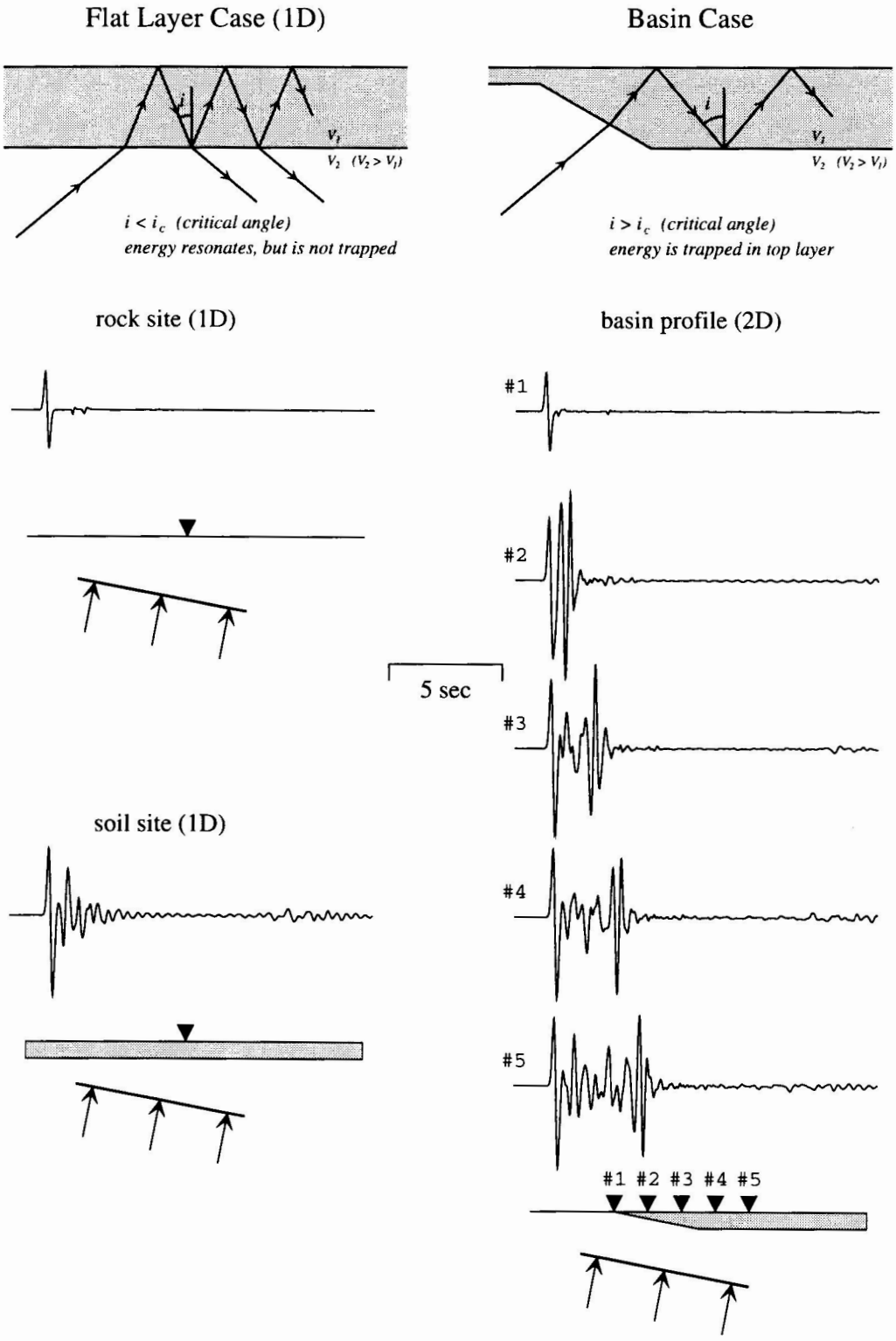

Figure 6. Schematic diagram showing that seismic waves entering a sedimentary layer from below will resonate within the layer but escape if the layer is flat (left) but become trapped in the layer if it has varying thickness and the waves enter it through its edge (right). Source: Graves, 1993.

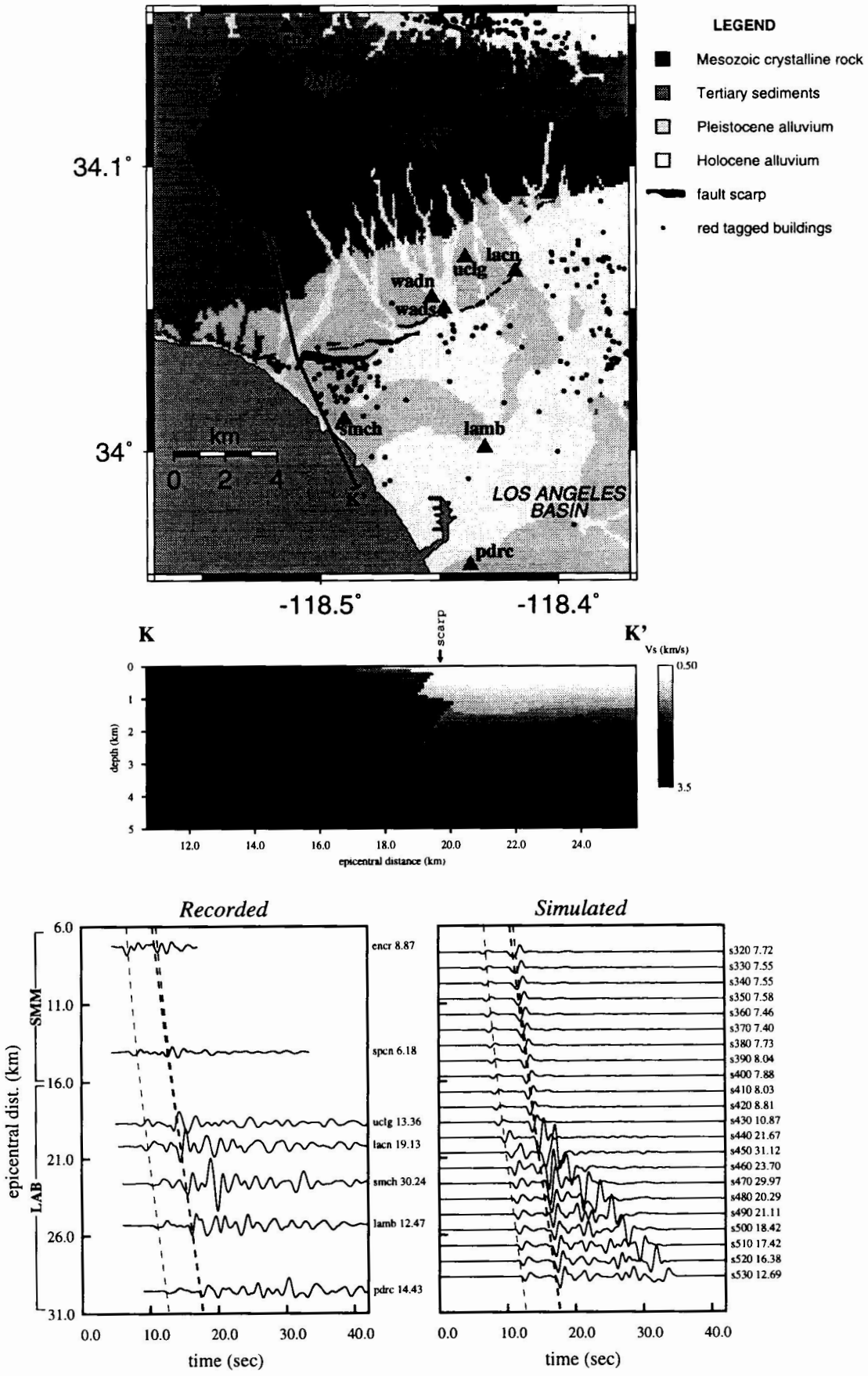

Figure 7. Basin effects in Santa Monica from the 1994 Northridge earthquake. See text for explanation. Source: Graves et al., 1998.

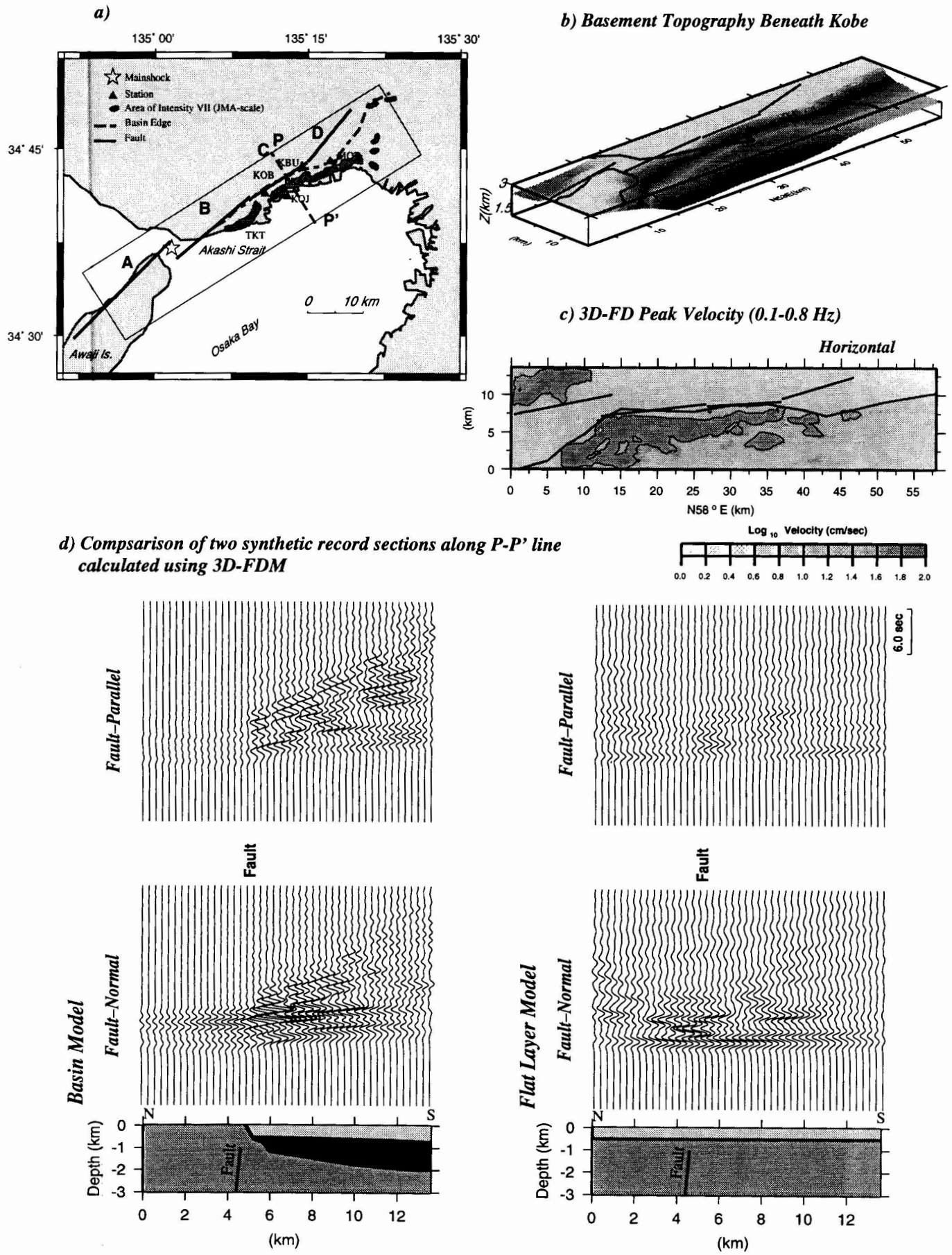

Figure 8. Basin edge effects in the 1995 Kobe earthquake. See text for explanation. Source: Pitarka et al., 1998.

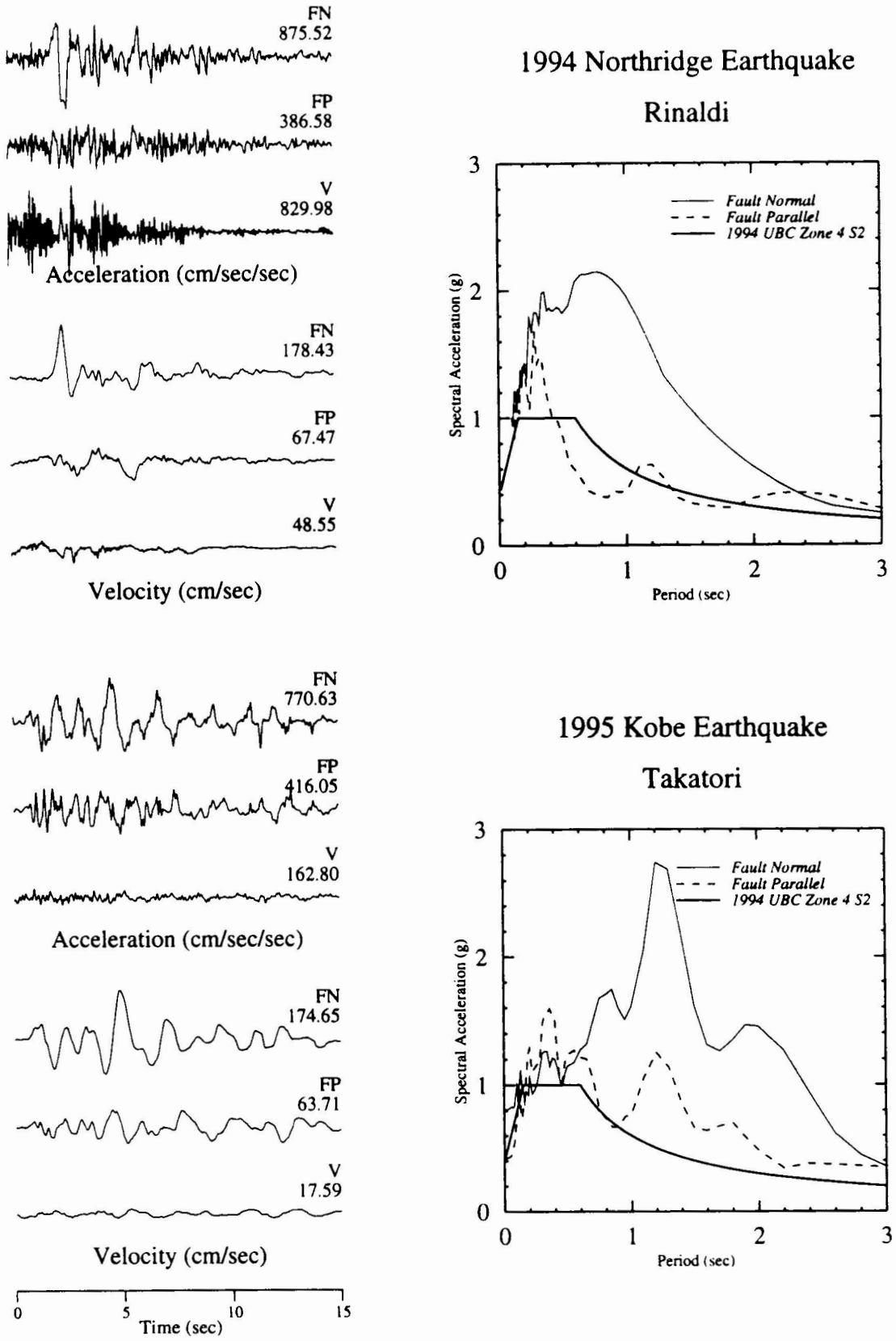

Figure 9. Recorded near-fault acceleration and velocity time histories and acceleration response spectra of the 1994 Northridge earthquake (top) and 1995 Kobe earthquake (bottom), showing pulse-like motion on the fault-normal component of motion, which is much larger than the fault-parallel component at periods longer than about 0.5 seconds. The 1994 UBC code spectrum for Zone 4, S2 soil conditions is shown for reference.